

IMAC fractionation in combination to LC/MS reveals H2B and NIF-1 peptides as potential bladder cancer biomarkers

Maria Frantzi, Jerome Zoidakis, Theofilos Papadopoulos, Petra Zurbig, Ioannis Katafigiotis, Konstantinos Stravodimos, Andreas Lazaris, Ioanna Giannopoulou, Achilles Ploumidis, Harald Mischak, William (Bill) Mullen, and Antonia Vlahou

J. Proteome Res., **Just Accepted Manuscript** • DOI: 10.1021/pr400255h • Publication Date (Web): 07 Aug 2013

Downloaded from <http://pubs.acs.org> on August 13, 2013

Just Accepted

“Just Accepted” manuscripts have been peer-reviewed and accepted for publication. They are posted online prior to technical editing, formatting for publication and author proofing. The American Chemical Society provides “Just Accepted” as a free service to the research community to expedite the dissemination of scientific material as soon as possible after acceptance. “Just Accepted” manuscripts appear in full in PDF format accompanied by an HTML abstract. “Just Accepted” manuscripts have been fully peer reviewed, but should not be considered the official version of record. They are accessible to all readers and citable by the Digital Object Identifier (DOI®). “Just Accepted” is an optional service offered to authors. Therefore, the “Just Accepted” Web site may not include all articles that will be published in the journal. After a manuscript is technically edited and formatted, it will be removed from the “Just Accepted” Web site and published as an ASAP article. Note that technical editing may introduce minor changes to the manuscript text and/or graphics which could affect content, and all legal disclaimers and ethical guidelines that apply to the journal pertain. ACS cannot be held responsible for errors or consequences arising from the use of information contained in these “Just Accepted” manuscripts.



IMAC fractionation in combination to LC/MS reveals H2B and NIF-1 peptides as potential bladder cancer biomarkers

Maria Frantzi^{1,3}, Jerome Zoidakis¹, Theofilos Papadopoulos¹, Petra Zürgbig³, Ioannis Katafigiotis⁴, Konstantinos Stravodimos⁴, Andreas Lazaris⁵, Ioanna Giannopoulou⁵, Achilles Ploumidis⁶, Harald Mischak^{2,3}, William Mullen² and Antonia Vlahou^{1*}

¹Biomedical Research Foundation Academy of Athens, Greece

²Institute of Cardiovascular and Medical Sciences, University of Glasgow, United Kingdom

³Mosaiques diagnostics GmbH, Hannover, Germany

⁴1st Department of Urology, 'Laiko' General Hospital, University of Athens, School of Medicine

⁵1st Department of Pathology, University of Athens, School of Medicine, Athens, Greece

⁶Department of Urology, Athens Medical Centre, Athens, Greece

ABSTRACT

Improvement in bladder cancer (BC) management requires more effective diagnosis and/or prognosis of disease recurrence and progression. Urinary biomarkers attract special interest due to the non-invasive means of urine collection. Proteomic analysis of urine entails the adoption of a fractionation methodology to reduce sample complexity. In this study, we applied immobilized metal affinity chromatography in combination with high resolution LC-MS/MS for the discovery of native urinary peptides potentially associated with BC aggressiveness. This approach was employed towards urine samples from patients with invasive BC, non-invasive BC and benign urogenital diseases. 1845 peptides were identified,

1
2
3 25 corresponding to a total of 638 precursor proteins. Specific enrichment for proteins involved
4
5 26 in nucleosome assembly and for zinc-finger transcription factors was observed. The
6
7 27 differential expression of two candidate biomarkers, histone H2B and NIF-1 (zinc finger 335)
8
9 28 in BC, was verified in independent sets of urine samples by ELISA and by
10
11 29 immunohistochemical analysis of BC tissue. The results collectively support changes in the
12
13 30 expression of both of these proteins with tumour progression, suggesting their potential role
14
15 31 as markers for discriminating BC stages. Also, the data indicate a possible involvement of
16
17 32 NIF-1 in BC progression, likely as a suppressor and through interactions with Sox9 and
18
19 33 HoxA1.
20
21
22
23
24 34

25
26 35 **KEYWORDS:** urine, bladder cancer, peptidomics, NIF-1, H2B
27
28
29 36

30
31
32 37 **SIGNIFICANCE / NOVELTY**
33

34
35 38 This study provides an in-depth analysis of the urinary peptidome in association with bladder
36
37 39 cancer (BC). IMAC fractionation combined with LC-MS/MS was applied. Native urinary
38
39 40 peptides originating from histones and zinc-finger proteins, not yet detected in urine, were
40
41 41 enriched. Differential expression of H2B and NIF-1 with BC stage was further verified in
42
43 42 urine by ELISA and tissue by immunohistochemistry. We hypothesize an involvement of
44
45 43 NIF-1 in BC progression likely through interactions with Sox9.
46
47
48
49 44

45 INTRODUCTION

46 Bladder cancer (BC) is the second most frequent genitourinary malignancy after prostate
47 cancer¹. According to TNM criteria, urothelial cancers are classified into different stages: Ta
48 for non-invasive papillary carcinoma, Tis for carcinoma *in situ*, T1 for tumours that have
49 invaded the subepithelial connective tissue and stages T2-4 for muscle invasive cancers^{2, 3}.
50 Disease prognosis and BC treatment strategies are related to tumour stage and other clinico-
51 pathological characteristics⁴.

52 Currently the golden standard in BC initial diagnosis and surveillance is the histopathologic
53 analysis of biopsy specimens obtained by cystoscopy. Of the non-invasive methods, urinary
54 cytology is being applied, as adjunct to the cystoscopic evaluation, even though it is
55 associated with low sensitivity particularly in the detection of low grade disease⁵. Other
56 urinary molecular BC tests have been recently introduced into clinical practice, like NMP22,
57 UroVysion and Immunocyt. However, none of them could successfully replace cystoscopy as
58 a stand-alone test⁶. The main clinical needs for BC currently include development of non-
59 invasive, more accurate tests for initial diagnosis and surveillance. Main areas of applications
60 are the early detection/prognosis of disease recurrence and progression as well as prediction
61 of response to neoadjuvant and adjuvant therapies^{7, 8}.

62 Urine serves as a biomarker source for BC, not only because it is in direct contact with the
63 urinary tract, but also because it is easily and non-invasively accessible⁹. However, due to its
64 high complexity and high concentration of salts and interfering compounds, adoption of a
65 protein separation or enrichment step is required when targeting the discovery of new
66 biomarkers. We recently described the application of IMAC fractionation in combination to
67 “bottom-up” proteomics (e.g. tryptic digestion followed by LC/MS analysis) for the
68 enrichment of low abundance proteins in urine¹⁰. This approach proved to be an effective tool

1
2
3 69 for the isolation of matrix metalloproteinases and other proteases and proteins involved in
4
5 70 cytoskeletal rearrangement¹⁰. Among the latter, Profilin-1 was found to provide prognostic
6
7 71 information¹⁰. In this study, we focus on the naturally occurring urinary peptides in
8
9
10 72 association with BC stages, following enrichment with IMAC fractionation and a “top-down”
11
12 73 (e.g. lack of tryptic digestion) MS analysis. The clinical objective of the current study is, thus,
13
14 74 diagnostic with the ultimate goal to improve management of patients with BC. A clear
15
16 75 enrichment for peptides corresponding to Zn-finger proteins may be observed as well as for
17
18 76 nucleosomal proteins, -not yet included in existing urine peptidome databases, selectively
19
20 77 from cancer samples. The differential expression of histone H2B and Zn finger 335 (NIF-1)
21
22 78 in urine was further confirmed by ELISA analysis and initial evidence for the functional
23
24 79 relevance of these proteins was provided by immunohistochemistry of BC tissue sections.
25
26
27
28
29
30

80

31 **EXPERIMENTAL PROCEDURES**

32 **Urine sample collection, handling and storage**

33
34
35
36 83 Urine samples (random-catch) were collected in two centres: Laikon Hospital and
37
38 84 Asklepieion Voulas General Hospital both in Athens, Greece. Proper informed consent
39
40 85 procedures under Institutional Review Board approved protocols were followed. Samples
41
42 86 were collected according to the standard protocol for urine collection defined by the
43
44 87 European Kidney and Urine Proteomics (EuroKUP) and Human Kidney and Urine Proteome
45
46 88 Project (HKUPP) networks (<http://www.eurokup.org/node/138>) including freezing at -80°C
47
48 89 within 3h of collection and a brief centrifugation step prior to proteome analysis¹¹. Samples
49
50 90 were collected in between 2003-2012, therefore storage time differed per sample nevertheless
51
52 91 this was evenly distributed among groups.
53
54
55
56
57
58
59
60

92

93 Immobilized Metal Affinity Chromatography (IMAC)

94 IMAC chromatography was performed, as previously described¹⁰. IMAC uncharged resin
95 (Profinity-BioRad) was used to generate a 10mL chromatography column (BioRad)
96 according to the manufacturer's instructions. In brief, 0.5mL of resin was applied in the
97 column, washed with 8mL of deionized water, followed by a wash with 8mL of binding
98 buffer (50mM NaH₂PO₄, 300mM NaCl, 1mM Imidazole, pH 8). Prior to metal ion loading
99 (Ni²⁺), the column was equilibrated with 8mL of 50mM CH₃COONa, 300mM NaCl, pH 4. A
100 volume of 8mL 200mM NiSO₄, pH 6.8 was added and the column was washed again with
101 10mL of deionized water, followed by a wash with 8mL binding buffer (50mM NaH₂PO₄,
102 300mM NaCl, 1mM Imidazole, pH 8). One mg of total protein corresponding to 210 to 770
103 µl per sample) was mixed with binding buffer at a ratio of 1:4 respectively and applied to the
104 column. Several fractions of flow through were collected (2mL/fraction). The column was
105 then washed with 10mL of wash buffer (50mM NaH₂PO₄, 300mM NaCl, 5mM Imidazole,
106 pH 8), during which 5 fractions were collected (2mL/fraction) to monitor washing efficiency.
107 Elution was performed by the addition of 4mL elution buffer (50mM NaH₂PO₄, 300mM
108 NaCl, 500mM Imidazole, pH 8). Elution fractions were dialyzed (700Da cut-off) against 3L
109 of water. Following this dialysis step, eluates were dried by speedvac and resuspended in
110 100µl of HPLC grade H₂O. An aliquot was taken for LC-MS/MS analysis, as described
111 below. The remaining sample was stored at -80°C. IMAC was performed on individual urines
112 from patients with non-invasive (5 Ta and 5 T1) and invasive (5 T2+) BC and benign
113 urothelial diseases (n=5). Detailed clinical data per sample are provided in **Supplementary**

114 Table 1.

115
116
117

118 **LC-MS Analysis for Peptide Sequencing**

119 LC-MS analysis was performed using an Ultimate3000 nano-LC pump (Dionex, Camberley
120 UK) coupled to an Orbitrap LTQ-Velos FTMS via Proxeon nano spray source (Thermo
121 Fisher, Hemel, UK). 5 μ L were loaded onto a Dionex 100 μ m x 2 cm 5 μ m C18 nano trap
122 column and separated on a Dionex C18 reverse phase column (75 μ m ID \times 150 mm, 100 \AA).
123 Peptides were eluted using a gradient of 1-5-40% B (80% ACN, 0.1% formic acid) in 0-5-60
124 min at a flow rate of 300 nL / min. The eluate from the column was directed to the Thermo
125 Proxeon nano spray ESI source operating in positive ion mode then into the Orbitrap LTQ
126 Velos FTMS. The ionisation voltage was 2.5 kV and the capillary temperature was 200 $^{\circ}$ C.
127 The mass spectrometer was operated in MS/MS mode scanning from 380 to 2000 amu. The
128 top 20 multiply charged ions were selected for MS/MS analysis using data dependant
129 dynamic exclusion. The repeat count was 1 and repeat duration 15 seconds, exclusion mass
130 widths were \pm 5 ppm. The fragmentation method was HCD at 35% collision energy. The
131 resolution of ions in MS1 was 60000 and 7.500 for HCD MS2.

132

133 **Data analysis**

134 Raw spectral data from LC-MS/MS analysis were uploaded to Thermo Proteome Discoverer
135 1.2. Peptides were considered if signal to noise ratio was higher than 1.5 and belonged to
136 precursor ions of 700 – 8000 Da. Peptide and protein identification was performed with
137 SEQUEST algorithm using Uniprot version 01052012 of human taxonomy. No enzyme
138 cleavage was selected and oxidation of methionine and hydroxylation of proline were chosen
139 as variable modifications. Precursor tolerance was set at 10 ppm and 0.1 Da for MS/MS
140 fragment ions. Resulting peptides and protein hits were further screened by accepting only
141 those hits listed as high confidence by the Proteome Discoverer software. FDR was estimated
142 to be 0.4%.

1
2
3 1434
5 144 **ELISA**

6
7 145 For the investigation of H2B and NIF-1 levels in individual urine samples, commercially
8
9 146 available ELISA Kits from USCN LIFE, INC. were employed. A total of 166 individual
10
11 147 urine samples from patients with benign diseases of the urogenital tract (BPH, inflammation,
12
13 148 lithiasis, hematuria), patients with Ta BC, T1 BC and invasive T2+ urothelial carcinoma were
14
15 149 employed (demographics and clinical information per sample are available in
16
17 150 **Supplementary Table 1**). H2B levels in urine were determined in a total of 147 urine
18
19 151 samples: 39 benign, 40 Ta, 36 T1 and 32 T2+. NIF-1 was quantified in a total of 158 urine
20
21 152 samples: 47 benign, 44 Ta, 36 T1 and 31 T2+ (all raw data-measurements per sample are
22
23 153 provided in **Supplementary Table 3**). The assays were performed according to the
24
25 154 manufacturer's instructions using 100µl of urine per well. The NIF-1 kit was approved and
26
27 155 validated for use in urine by the manufacturer. In the case of the H2B kit, a negative urine
28
29 156 sample was spiked with all the H2B standards and in all cases the H2B measurements were
30
31 157 very close to the expected ones ($R^2 = 0.9931$, standards used: 0.039, 0.078, 0.156, 0.312,
32
33 158 0.625, 1.25, 2.5 ng/ml; data not shown). For all samples with concentration <LOQ, "0" values
34
35 159 were used for statistical analysis.

36
37
38
39
40 16041
42
43 161 **Immunohistochemistry**

44
45 162 Formalin-fixed tissue specimens from a total of thirty two patients [mean age at diagnosis
46
47 163 67.1 years (age range: 50–86 years); 27-male, 5-female; **Supplementary Table 1**] with BC
48
49 164 were employed for immunohistochemical analysis. These samples were obtained from first
50
51 165 transurethral resection of the bladder or through radical cysto-prostatectomies. Sections were
52
53 166 evaluated with hematoxylin-eosin stain and graded according to the WHO 1973 and
54
55 167 WHO/ISUP (2004) as grade 1 (5 cases), grade 2 (13 cases), grade 3 (14 cases) and as low-

1
2
3 168 grade (17 cases) and high-grade papillary urothelial carcinomas (15 cases), respectively.

4
5 169 Staging was performed according to TNM/UICC(2009) classification³, as follows: pTa (11
6
7 170 cases), pT1 (12 cases), pT2 (5 cases), pT3 (2 cases) and pT4 (2 cases). In situ carcinoma co-
8
9 171 existed in 6 cases.

10
11 172 Immunohistochemical staining for Histone2B and NIF-1 was performed on 4 μ m thick
12
13 173 formalin-fixed paraffin sections. To enhance antigen retrieval, sections were microwave-
14
15 174 treated in 10 mM citrate buffer, pH 6.0 at 750W for three cycles of 5min each. This protocol
16
17 175 was selected following initial optimization experiments, during which antigen retrieval with
18
19 176 different buffers (10 mM citrate buffer pH 6.0 or 1 mM EDTA pH 8.0), or without antigen
20
21 177 retrieval were performed. As positive controls for both H2B and NIF-1,
22
23 178 immunohistochemistry of paraffin-embedded human breast carcinoma tissues were used.
24
25 179 Negative controls had the primary antibody omitted and replaced by non-immune normal
26
27 180 serum from the same species. Endogenous peroxidase activity was quenched with 0.3%
28
29 181 hydrogen peroxide in Tris-buffered saline (TBS). After rinsing with TBS, normal horse
30
31 182 serum was applied for 30 minutes to block non-specific antibody binding. Subsequently,
32
33 183 sections were incubated overnight at 4 °C with the following antibodies: a rabbit monoclonal
34
35 184 antibody against Histone2B (clone EP957Y, Millipore, Temecula, CA, USA), diluted 1:500
36
37 185 and a rabbit polyclonal antibody against NIF-1 (cat.No.IHC-00194, Bethyl Laboratories,
38
39 186 Montgomery, TX, USA) diluted 1:80.

40
41 187 A three-step technique (Avidin-Biotin-Peroxidase, Vector Laboratories, Burlingame, CA,
42
43 188 USA) was used for visualization, with diaminobenzidine as a chromogen according to the kit
44
45 189 instructions. Finally, sections were counterstained with hematoxylin and mounted.
46
47
48
49
50
51

52 190

53 191

54 192

193 **Evaluation of Immunohistochemistry**

194 Evaluation of the immunohistochemical staining was performed independently by two
195 pathologists (AL, IG) without knowledge of the clinical data for each patient. Through this
196 initial manual analysis no spurious staining and a homogeneous pattern of expression for the
197 two proteins throughout the epithelial cells in the section were in general observed. A score
198 per section was assigned according to the number of positive cells and staining intensity.
199 Specimens were scored as 0: negative, 1+: low, 2+: moderate, 3+: intense expression (data
200 not shown). Nuclear immunoreactivity for H2B and nuclear-cytoplasmic immunoreactivity
201 for NIF-1 were observed.

202 To assess the samples independent from the visual inspection, which may be subject to
203 observer bias, an image analysis approach was implemented using the Image J software that
204 enables analysis of a RGB image in separate channels, as described by Ruifrok and
205 collaborators¹². Briefly, every tissue section was scanned under the microscope using X20
206 magnification. Depending on tissue size, 5-10 images were acquired per section. For each
207 image, 10-50 fields of identical area dimensions (16200nm²) were selected to be measured.
208 Optical density was normalized over the tissue substrate which was employed as negative
209 background. Mean values of intensity were calculated per image and subsequently for each
210 section (tissue sample). All raw data-measurements per sample are provided in

211 **Supplementary Table 3.**

213 **Statistical Analysis**

214 Statistical analysis was performed using the SPSS statistical software (SPSS 17.0: IBM). The
215 Kolmogorov – Smirnov test (K-S test) was employed to test for normal data distribution. In

1
2
3 216 case that data normality could not be demonstrated, the Mann-Whitney test was applied,
4
5 217 whereas in cases of normal distribution the t-test was used. In all cases, $p < 0.05$ was
6
7 218 considered statistically significant. The boxplots were created by the use of the Origin
8
9 219 software (OriginPro v.8: OriginLab Corporations). Correlations between biomarker levels and
10
11 220 urinary protein content were investigated using the Spearman's rho and Pearson correlation
12
13 221 tests.
14
15
16
17 222

20 223 **RESULTS**

21
22
23 224

25 225 **Workflow for biomarker discovery**

26
27 226 To enrich for potential BC urinary biomarkers, a proteomics approach was utilized
28
29 227 combining a fractionation methodology coupled to LC-MS/MS. IMAC-Ni was used to
30
31 228 reduce complexity, while allowing for the selective enrichment of metal binding proteins.
32
33 229 Five samples per category (benign, non-invasive T_a and T₁, invasive T₂+) were fractionated.
34
35 230 As this methodology is cumbersome and of low reproducibility, the received protein
36
37 231 identifications per sample were compiled to form a list of identifications per category e.g.
38
39 232 benign, non invasive, invasive, representing the sum of identifications of all samples in the
40
41 233 respective group). Comparison of different groups was then conducted in a qualitative
42
43 234 manner and findings were prioritized based on the following parameters: a) strength of
44
45 235 evidence for differential expression (number of samples where the peptide was present); b)
46
47 236 (parental) protein functional annotation; c) potential relevance to bladder cancer invasion.
48
49 237 Following this procedure the presented identifications and respective differences (based on
50
51 238 presence-absence) between groups cannot be considered as "significant changes". However,
52
53 239 this list in combination with a thorough protein functional annotation and literature mining,
54
55
56
57
58
59
60

1
2
3 240 becomes *suggestive* of potential disease related biomarkers, meriting further investigation.

4
5 241 Among the latter, two proteins, Zinc-Finger 335 (NIF-1) and H2B were selected for further

6
7 242 validation by antibody –based assays in independent sets of urine and tissue samples. A

8
9 243 schematic representation of this study design and workflow is depicted in **Figure 1**.

10
11 244

12 13 14 15 245 **IMAC fractionation provides enrichment of naturally occurring urinary peptides**

16
17 246 The received 1845 peptide identifications from LC-MS/MS analysis of the eluted fractions

18
19 247 incorporating stringent identification criteria, corresponded to 638 distinct precursor proteins

20
21 248 in total (**Supplementary Table 2**). Common identifications (46 precursor proteins) with the

22
23 249 existing urine peptidome database¹³ involved mainly serum proteins like Haemoglobin

24
25 250 subunits, Immunoglobulin chains, Albumin, Plasma protease inhibitors, Apolipoprotein

26
27 251 isoforms, Complement components, and Transthyretin, as well as Collagen and Fibrinogen

28
29 252 fragments and others (e.g. Osteopontin, Gelsolin, Protein S100-A9, etc). The enrichment for

30
31 253 many of these proteins was expected due to their affinity for metal ions (e.g. Albumin,

32
33 254 Serotransferrin etc). Interestingly, 592/638 proteins or 92.8% of our identifications had not

34
35 255 been previously detected in unfractionated urine¹³. This is likely due to their low abundance,

36
37 256 and may indicate good efficiency of the enrichment strategy. Metal affinity chromatography

38
39 257 using Ni²⁺ as an immobilized ligand is an efficient strategy for the purification of proteins

40
41 258 with C₂H₂ zinc-finger domains¹⁴ and/or being phosphorylated¹⁵. Nevertheless, as shown

42
43 259 (**Supplementary Table 2**) the affinity of the identified peptides for the IMAC Ni column

44
45 260 cannot be readily attributed to these factors (e.g. metal binding and phosphorylation). Since

46
47 261 Histidine (H), Arginine (R) or Lysine (K) are amino acids that show affinity for Ni²⁺ ¹⁶,

48
49 262 peptides containing these amino acids may also bind to the IMAC column. In fact, 94% of the

50
51 263 identified peptides contain at least one of Histidine (H), Arginine (R) or Lysine (K).

52
53 264

54
55
56
57
58
59
60

1
2
3 265 **Functional Annotation of the peptidomics data reveals a high number of nucleosome**
4
5 266 **assembly and Zn finger transcription factors in bladder cancer urine samples.**
6

7 267

8
9
10 268 “In silico” evaluation of the findings for their biological significance was conducted using a
11
12 269 combination of GO analysis, text mining, as well as search through expression databases such
13
14 270 as the Human Protein Atlas database (www.proteinatlas.org). **Figure 2** illustrates the
15
16 271 distribution of received identifications, according to the protein biological function (similar
17
18 272 distribution was received within each individual group, e.g. invasive, non-invasive and
19
20 273 benign- data not shown).

21
22
23 274 As shown, various identified proteins are immunological components, such as proteins
24
25 275 involved in complement activation, cytokine signalling and inflammation. A substantial part
26
27 276 of identifications consist of proteins involved in signalling pathways: such as Ras-related
28
29 277 proteins, G-protein signalling modulators and Rho-related GTP-binding proteins
30
31 278 (Puratrophin-1, Kalirin and Tuberin). Other peptide identifications correspond to proteins
32
33 279 with demonstrated function in cytoskeleton remodelling and cell adhesion rearrangements:
34
35 280 e.g. Gelsolin, Slit homolog 2, Slit homolog 3, and its receptor Roundabout 4, all known to
36
37 281 regulate actin polymerization. Proteins involved in oxidative stress response were also
38
39 282 enriched, such as, Peroxiredoxin-2 (Natural killer cell-enhancing factor B) and Glutathione S-
40
41 283 Transferase P as well as proteins involved in apoptosis, (Anamorsin or Cytokine-induced
42
43 284 apoptosis inhibitor 1 etc.).

44
45
46
47
48 285 Interestingly, an over-representation in the cancer samples of peptides related to nuclear-
49
50 286 nucleosomal proteins was observed (such as many peptides deriving from Histones) as well
51
52 287 as of Zn finger transcription factors (**Supplementary Table 2**). Taking this into account and
53
54 288 in combination with the novelty of these initial findings, as well as antibody availability, we
55
56
57
58
59
60

1
2
3 289 opted to further investigate the value of histone H2B and Zinc finger 335 (NIF-1) as potential
4
5 290 biomarkers for bladder cancer.
6

7 291

8
9
10 292 **ELISA analysis in urine samples confirms mass spectrometric results**

11
12 293 The urinary protein levels for NIF-1 and H2B were quantified by ELISA in independent sets
13
14 294 of individual urine samples (detailed data per sample are provided in **Supplementary Table**
15
16
17 295 **3**).

18
19 296 A total of 158 urine samples were analysed for NIF-1: 47 samples from patients with benign
20
21 297 urothelial diseases, 44 from patients with Ta, 36 from T1 and 31 from T2+ BC. In the vast
22
23 298 majority of urine samples, NIF-1 could be detected, as shown by the number of positive
24
25 299 samples: In total, 106/111 (or 95.9%) cancer cases were positive for NIF-1. The mean values
26
27 300 and standard deviation of NIF-1 levels are summarized in **Figure 3A**. Progressively
28
29 301 increasing levels of urinary NIF-1 are observed with increasing tumour stage. In general, the
30
31 302 levels of NIF-1 did not follow normal distribution (according to the K-S test, data not
32
33 303 shown), therefore, the Mann- Witney test was applied to estimate statistical significance. This
34
35 304 analysis showed significant differences between the NIF-1 levels in the benign samples
36
37 305 compared to the cancer groups (B vs. Ta $p=0.043$), (B vs. T1 $p=0.018$) (B vs. T2+
38
39 306 $p=0.0000062$). In addition, the T2+ exhibited a significant increase compared to non-invasive
40
41 307 Ta (Ta vs. T2+ $p= 0.014$), although the difference between T1 and T2+ was not statistically
42
43 308 significant. This trend of expression was also observed when the ELISA data were
44
45 309 normalized according to creatinine (**Supplementary Table 3**).

46
47
48
49 310 For H2B, 147 urine samples were analysed by ELISA. In this case, larger variations
50
51 311 (compared to NIF-1) in the number of positive samples per group could be observed:
52
53 312 Detectable levels for H2B were observed in 15 out of 39 (38.5%) benign samples, 35 out of
54
55 313 40 (87.5%) Ta samples, 19 out of 36 (52.8%) T1 and 23 out of 32 (71.9%) T2+ samples.
56
57
58
59
60

1
2
3 314 When considering the levels of expression (summarized in **Figure 3B**), H2B was found at
4
5 315 significantly higher levels in the cancers compared to the benign samples (Benign vs. Ta
6
7 316 $p=0.0000046$, Benign vs. T1 $p=0.042$, Benign vs. T2+ $p=0.001$ according to Mann Whitney;
8
9 317 **Figure 3B**). Between the cancer categories, statistically significant difference was found only
10
11 318 for Ta vs. T1 pair sets (Ta vs. T1 $p=0.033$ -Mann Whitney). As in the case of NIF-1, this
12
13 319 observed trend of expression was not affected by data normalization according to creatinine.
14
15 320 However, when the normalization was calculated over the total protein, these trends of
16
17 321 expression with tumour stage could no longer be detected for neither H2B nor NIF-1
18
19 322 (**Supplementary Table 3**). This attenuation of urinary biomarker changes when normalized
20
21 323 according to total protein in bladder cancer is in line to recent reports¹⁷.
22
23 324

24 25 26 27 325 **Differential expression of NIF-1 and H2B in BC tissue sections**

28
29
30 326 The results from the urine analysis prompted a further investigation of the association of NIF-
31
32 327 1 and H2B with BC at the tissue level. Towards that end, immunohistochemical analysis of
33
34 328 BC tissue specimens was performed. A colour deconvolution image analysis method (Image
35
36 329 J software) was implemented to allow for a more accurate and objective signal quantification.
37
38 330 The results of this analysis were overall in accordance to the scoring provided by the
39
40 331 pathologists (data not shown). Twenty-eight sections were stained for NIF-1 divided in 3 BC
41
42 332 groups, 11 Ta, 10 T1 and 8 T2+. Five to ten (depending on the tissue section size)
43
44 333 representative images were selected from each section (average number of images per sample
45
46 334 was 7 for Ta, 7 for T1 and 5 for T2+; raw data are provided in **Supplementary Table 3**).
47
48 335 Nuclear, as well as, cytosolic NIF-1 expression was observed in a relative homogeneous
49
50 336 pattern among epithelial cells per section (**Supplementary Table 3**). Deviations from the
51
52 337 mean corresponded to images containing lower number of epithelial cells and/or occasionally
53
54 338 epithelial cells of different morphology (**Supplementary Figure**) suggesting that these may
55
56
57
58
59
60

1
2
3 339 represent different stages in the disease evolution. Quantification of the IHC intensity
4
5 340 revealed a clear overall reduction of NIF-1 expression as cancer stage progresses (**Figure**
6
7 341 **4A**). Statistical analysis of the received optical density (OD) values supported a significant
8
9 342 difference between non-invasive (Ta, T1) and invasive (T2+) cancers (Ta vs. T1 $p=0.191$ for
10
11 343 Ta vs. T2+ $p=4.5E-6$ and T1 vs. T2+ $p=0.001$ according to t-test (normality was predicted
12
13 344 based on the K-S test). Mean value (SD) per stage and respective raw data are provided in
14
15
16 345 **Supplementary Table 3**.

17
18
19 346 In the case of H2B, the same quantification strategy was applied. Nuclear staining was
20
21 347 observed which, similarly to NIF-1, exhibited a relative homogeneous staining throughout the
22
23 348 section in areas of similar tissue and cell morphology. Occasionally, epithelial cells were
24
25 349 found to differ in their intensity measurements within the same section (representative images
26
27 350 are also presented in **Supplementary Figure**) likely attributed to differences in the degree of
28
29 351 aggressiveness. A difference in the overall staining intensity between the three cancer
30
31 352 categories could be observed (**Figure 4B**). However, in contrast to NIF-1, the OD increases
32
33 353 with increasing cancer stage. A statistically significant difference was observed between the
34
35 354 non-invasive (Ta, T1) and T2+ invasive BC (Ta vs. T2+ $p=0.001$ and T1 vs. T2+ $p=0.009$)
36
37 355 whereas no significant difference was observed between the non-invasive Ta and T1 cancers
38
39 356 (Ta vs. T1 $p=0.998$; in all cases, the t –test was applied as OD data followed normal
40
41 357 distribution according to the K-S test). Mean value (SD) per stage and respective raw data are
42
43 358 provided in **Supplementary Table 3**.

44
45
46
47
48
49 359 Collectively, these results supported an association of NIF-1 and H2B tissue levels with
50
51 360 tumour stage (even though with opposing trends of expression: decreased levels for NIF-1
52
53 361 and increased for H2B in the invasive versus non-invasive groups).
54
55
56
57
58
59
60

1
2
3 362 No further associations of H2B to histological grade were observed. In the case of NIF-1,
4
5 363 immunoreactivity was inversely associated with tumour grade (WHO 2004 classification
6
7 364 $p=0.013$). Using the WHO 1973 grading system, NIF-1 expression displayed a significant
8
9
10 365 negative correlation between grade 2 and grade 3 carcinomas ($p=0.003$) (**Supplementary**
11
12 366 **Table 3**).

13
14
15 367 H2B and NIF-1 have been found to interact with each other¹⁸. The existence of possible
16
17 368 correlation between the OD values of the two proteins was also investigated by the
18
19 369 performance of a curve estimation (**Table 1**). A statistically significant correlation ($p= 0.036$)
20
21 370 following an inversely proportional with a Pearson Correlation value -0.391 was received,
22
23 371 suggesting that as H2B levels increase with tumour stage, and NIF-1 levels decrease.

24
25
26
27 372

28 29 373 **DISCUSSION**

30
31 374 Bladder cancer is a malignancy of particular interest for clinical proteomics approaches due
32
33 375 to increased tumour heterogeneity, high recurrence and progression rates, and lack of
34
35 376 effective non-invasive diagnostic and prognostic tools. Urine as a biological fluid has the
36
37 377 advantage of being easily and non-invasively obtained. To reduce sample complexity
38
39 378 allowing for efficient biomarker discovery, the application of enrichment strategies is a
40
41 379 frequently and successfully applied approach¹⁹. IMAC has been used to enrich for intact
42
43 380 proteins and peptides with high affinity to metal ions²⁰ and in phosphoproteomic studies^{21, 22}.
44
45 381 We previously applied this strategy to study urinary proteins associated with BC¹⁰. In that
46
47 382 case, the enriched proteins were analysed following SDS-PAGE of the IMAC eluted fractions
48
49 383 and tryptic digestion of the excised bands. In the present study, we focused on the low
50
51 384 molecular weight proteome using a gel-free approach that did not involve tryptic digestion
52
53
54
55 385 prior to the MS analysis.
56
57
58
59
60

1
2
3 386 We were able to detect peptides from 638 different proteins. In reference to the existing
4
5 387 peptide database¹³ which has been generated from >9,000 datasets, 46 out of the previously
6
7 388 reported 115 precursor proteins were also represented in the IMAC peptide eluates. As
8
9
10 389 aforementioned (results), these included many plasma and matrix structural proteins.
11
12 390 Interestingly, many of the 592 proteins not reported in the peptide database and representing
13
14 391 a wide variety of cellular pathways have been reported to be involved in BC and/or have
15
16 392 already been evaluated as BC biomarkers:

17
18
19
20 393 Urinary Fibrinogen fragments²³, Peroxiredoxin^{24, 25}, Tenascin²⁶, have all been associated
21
22 394 with specific BC phenotypes. Similarly, urinary Apolipoprotein A-II, Ceruloplasmin and
23
24 395 Complement C4 were found to be over-represented in BC²⁷. Hyaluronidase activity²⁸ and
25
26 396 TGF-beta²⁹ have also been investigated in association with BC. Moreover, Ceruloplasmin,
27
28 397 Dipeptidyl peptidase, Aminopeptidase isoforms, Leukine-rich alpha-2 glycoprotein are some
29
30 398 of the proteins that were also selectively enriched from BC samples in our previous IMAC
31
32 399 study involving analysis of the urinary (higher molecular mass) proteome¹⁰.

33
34
35
36 400 Of the urinary proteins, selectively enriched in BC samples, several have also been associated
37
38 401 with BC at the cell and/or tissue level: GST isoforms were suggested as BC
39
40 402 immunocytochemical markers to increase diagnostic accuracy of urine cytology³⁰. S100A9
41
42 403 has been suggested as a prognostic marker for invasive BC following microarray analysis³¹,
43
44 404 and Thymosin beta -4 was found up-regulated in BC by tissue microarrays³². In addition,
45
46 405 Tumour protein 63 identified in T1 BC samples in our series, has been reported to negatively
47
48 406 regulate EMT and metastasis in BC³³; Y-box-binding protein 2 identified in T2+ BC samples
49
50 407 promotes BC progression³⁴ and NKG2D ligand 1 is presumably involved in the inhibition of
51
52 408 tumour growth during BC treatment with BCG³⁵. Collectively, these results support the
53
54 409 efficiency of the proteomics strategy to enrich for proteins of relevance to BC.
55
56
57
58
59
60

1
2
3 410 Among the most prominent peptides detected were fragments from histone isoforms and
4
5 411 histone regulators: Multiple peptides of Histone H4, H2A and H2B were identified in BC
6
7 412 urines. Additionally, proteins involved in histone modifications and regulation were also
8
9 413 enriched, such as Histone-lysine N-methyltransferase SETD1A, POU domain-class 2
10
11 414 involved in histone H2B transcription³⁶ and Histone acetyltransferase p300. The latter is
12
13 415 associated with DNA damage response, resulting in alterations of H2A.X, mainly through
14
15 416 Bromodomain adjacent to zinc finger domain protein-2B³⁷, a protein which was also
16
17 417 identified in our study. Another related protein is NIF-1 (NRC-interacting factor; Zn finger
18
19 418 335). NIF-1 seems to act as a key molecule between two sub-complexes: one that displays
20
21 419 histone methyltransferase activity and another that is involved in nuclear receptor-mediated
22
23 420 transcription^{18, 38}. This dual action promotes the expression of several transcription factors^{18,}
24
25 421 ³⁹ among which HoxA1 and Sox9^{18, 40}, as supported by siRNA studies.

26
27
28
29
30 422 Based on this evidence supporting a functional association of H2B and NIF-1, in combination
31
32 423 with a lack of prior studies of these proteins in BC, H2B and NIF-1 were selected to be
33
34 424 further evaluated using immunological-based assays. Increased urinary levels for these
35
36 425 proteins were observed in the presence of urothelial carcinoma. The most aggressive T1 and
37
38 426 T2+ groups exhibit the highest levels of NIF-1 and Histone H2B. Nevertheless, we should
39
40 427 note that no direct (per sample) correlation between the discovery set (LC-MS data) and
41
42 428 verification set (ELISA data) could be observed as the two proteins were not detected in the
43
44 429 benign and non-invasive samples in the former (discovery) whereas the ELISA assays
45
46 430 demonstrated that some of these samples did contain detectable amounts of the respective
47
48 431 proteins (**Supplementary Table 3**). Given the low number of samples in the discovery set
49
50 432 and the high technical variability associated with IMAC fractionation, statistically
51
52 433 meaningful comparison between the LC-MS and the ELISA data is not possible. The high
53
54 434 inter-individual variability, particularly in the case of H2B, should also be noted, supporting
55
56
57
58
59
60

1
2
3 435 the presence of co-founders affecting the levels of these urinary proteins. Hematuria does not
4
5 436 appear to affect NIF-1 and H2B measurements based on the samples analysed, even though
6
7 437 analysis of a larger number of samples will be required to confirm this initial observation. In
8
9 438 addition, no correlations between the NIF-1/H2B levels and total urinary protein could be
10
11 439 observed ($p > 0.3$ in all cases according to Pearson and Spearman's rho correlation tests).

12
13 440 The fact that normalization to total protein was found to affect the value of H2B and NIF-1 as
14
15 441 biomarkers may relate to the association of bladder cancer with increased protein in urine⁴¹,
16
17 442 ⁴², rendering normalization according to protein inappropriate for this disease, as also
18
19 443 supported by recent publications¹⁷. Moreover, we should note that even though an initial
20
21 444 characterization of the performed assays was conducted (as described in the materials and
22
23 445 methods), the need for further characterization of the assays including an accurate
24
25 446 determination of LOQ, linear range for quantification, matrix effects etc. according to
26
27 447 regulatory requirements is required for clinical implementation^{43, 44}. In addition, even though
28
29 448 recognition of the expected protein bands is confirmed by the manufacturer, further
30
31 449 investigation of the antibody specificity including a detailed characterization of potential
32
33 450 isoforms of the two proteins in urine is required.

34
35
36
37
38
39 451 At the tissue level, a clearer pattern was received, strongly suggesting the association of these
40
41 452 proteins with BC stage. In this case, NIF-1 expression decreases, whereas H2B increases with
42
43 453 progressing tumour stage. The tissue H2B data are in good agreement to the urine H2B
44
45 454 expression pattern. This observation can probably be explained in part by the polyploidy
46
47 455 frequently observed in neoplastic cells, resulting in increased histone levels.

48
49
50
51 456 In the case of NIF-1, opposing trends of expression between the tissue (decrease in T2
52
53 457 cancers) and urine (increase in T2 cancers) are observed. The reason for this observation is
54
55 458 unknown at present. One possible explanation could be that with progression to advanced
56
57 459 stages the number of shed cancer cells increases substantially in the urine of patients.

1
2
3 460 Therefore, although NIF-1 production per cell is reduced, the urinary concentration of the
4
5 461 protein increases. Further experiments are required to test this hypothesis, including an
6
7 462 investigation of urine and tissue samples from the same patient.
8

9
10 463 Our current knowledge on NIF-1 is limited; in addition, no NIF-1 correlations to any type of
11
12 464 cancer have been reported. However, it should be noted that our observations appear to match
13
14 465 well with reported expression patterns of the NIF-1 direct targets, Sox9 and HoxA1: both
15
16 466 factors show negative or weak expression levels in urothelial cancer according to the Human
17
18 467 Protein Atlas (www.Proteinatlas.org), in which appears to be a tissue-specific pattern. This
19
20 468 preliminary evidence suggests a functional involvement of NIF-1 in combination with Sox9
21
22 469 and HOXA1 in BC tumour progression. Specifically, we may hypothesize that loss of NIF-1
23
24 470 expression leads to BC progression through silencing of Sox9, a transcription factor that
25
26 471 binds CDKN1A (cyclin-dependent kinase inhibitor 1A) promoter and inhibits cell growth in
27
28 472 vivo⁴⁰. Alternative mechanisms may include interactions of NIF-1 with other tumour
29
30 473 suppressors like DBC-1¹⁸. In these aggressive states where polyploidy is observed, in contrast
31
32 474 to NIF-1, H2B levels are elevated, reflected in the observed NIF-1/ H2B inverse association.
33
34 475 NIF-1 could also be associated with H2B regulation at the epigenetic level, either by its
35
36 476 integral methyltransferase activity or through interactions with ASCOM (NRC-
37
38 477 methyltransferase) complex¹⁸. Under hormone induction, alterations of H3 methylation status
39
40 478 could cause H2B/H2A rearrangements and nucleosome displacement⁴⁵.
41
42
43
44
45

46 479 Collectively, the presented study has enriched our knowledge on the peptidome of human
47
48 480 urine and more importantly, has revealed novel potential biomarkers such as NIF-1, possibly
49
50 481 of functional relevance in BC progression. This study thus opens up many new avenues of
51
52 482 research targeting, validation of the differential expression of these proteins in BC and
53
54 483 investigation of their specific context of use. **Table 2** highlights additional promising
55
56 484 candidates from our findings, selected based on their potential functional relevance and
57
58
59
60

1
2
3 485 existing knowledge in the field. Moreover the confirmation of the built hypothesis on NIF-
4
5 486 1/Sox9 involvement in BC progression as well as investigation of the proteolytic mechanisms
6
7 487 leading to the generation of the reported urinary peptides from their precursor proteins in
8
9
10 488 relation to disease progression warrant further investigation.

11
12
13 489
14
15
16
17
18
19
20
21
22
23
24
25
26
27
28
29
30
31
32
33
34
35
36
37
38
39
40
41
42
43
44
45
46
47
48
49
50
51
52
53
54
55
56
57
58
59
60

1
2
3 490 **ACKNOWLEDGEMENTS**
4

5
6 491 This work was supported in part by Marie Curie EID program BC MolMed (PITN-GA-2012-
7
8 492 31750), and Eu FP7 DECanBio (201333). All mass spectrometry data have been uploaded to
9
10 493 Human Protein Pedia (Proteinpedia ID: HuPA_00709).
11
12

13
14 494

15
16
17 495

18
19
20 496 **AUTHOR INFORMATION**
21

22 497 **Corresponding Author**
23

24
25 498 * Telephone: 30 210 65 97 506, fax: 30 210 65 97 545
26
27

28 499 Email: vlahoua@bioacademy.gr
29
30

31
32 500

33
34
35 501 **NOTE**
36

37 502 H. Mischak is founder and co-owner of Mosaiques Diagnostics, Germany and P. Zürgbig and
38
39 503 M. Frantzi are employed by Mosaiques Diagnostics. All other authors declare that they have
40
41
42 504 no competing interests.
43
44

45 505
46
47

48 506
49

50 507
51
52

53 508
54
55

56
57 509
58
59
60

510 **ABBREVIATIONS**

511 Ab: Antibody, ACN: Acetonitrile, amu: Atomic Mass Unit, ASCOM: Activating signal
512 cointegrator-2 complex, BC: Bladder Cancer, BCG: Bacillus Calmette-Guerin, BPH: Benign
513 prostatic hyperplasia, BTA: Bladder Tumour Antigen, CDKN1A: Cyclin-dependent kinase
514 inhibitor-1A, DBC: Deleted in Breast Cancer, ECM: Extracellular Matrix, ELISA: Enzyme-
515 linked immunosorbent assay, EMT: Epithelial to Mesenchymal Transition, ESI: Electrospray
516 Ionization, EuroKUP: European Kidney and Urine Proteomics, FTMS: Fourier Transform
517 Mass Spectrometry, GO: Gene Ontology, GTP: Guanosine Tri-Phosphate, H2B: Histone2B,
518 HCD: High energy Collision Dissociation, HKUPP: Human Kidney and Urine Proteome
519 Project, HOXA1: Homeobox A1, HPLC: High Performance Liquid Chromatography, IHC:
520 Immunohistochemistry, IMAC: Immobilized Metal Affinity Chromatography, IPI:
521 International Protein Index, LC: Liquid Chromatography, LTQ: linear trap quadrupole,
522 MRM: Multiple Reaction Monitoring, MS: Mass Spectrometry, NIF-1: NRC interacting
523 factor-1, NKG2D: Natural-killer group 2, member D, NMP22: Nuclear Matrix Protein 22,
524 NRC: Nuclear receptor coactivator, RGB: Red Green Blue, Robo: Roundabout homolog,
525 SDS PAGE: Sodium Dodecyl Sulfate Polyacrylamide Gel Electrophoresis, Sox9: Sex
526 determining region Y-box 9, SPSS Statistical Package For Social Sciences, TBS: Tris-
527 buffered saline, TNM: Tumour Nodes Metastases, WHO: World Health Organization, Zn:
528 Zinc.

529

530

531

532

533 REFERENCES

534

- 535 1. Ploeg, M.; Aben, K. K.; Kiemeny, L. A., The present and future burden of urinary bladder
536 cancer in the world. *World J Urol* **2009**, *27*, (3), 289-93.
- 537 2. Cheng, L.; Montironi, R.; Davidson, D. D.; Lopez-Beltran, A., Staging and reporting of
538 urothelial carcinoma of the urinary bladder. *Mod Pathol* **2009**, *22* Suppl 2, S70-95.
- 539 3. Sobin LH, G. M., Wittekind C; ; , TNM classification of malignant tumors. *UICC International*
540 *Union Against Cancer New York, NY: Wiley-Blackwell* **2009**, Ed7, p.262-5.
- 541 4. Shariat, S. F.; Chade, D. C.; Karakiewicz, P. I.; Ashfaq, R.; Isbarn, H.; Fradet, Y.; Bastian, P. J.;
542 Nielsen, M. E.; Capitanio, U.; Jeldres, C.; Montorsi, F.; Lerner, S. P.; Sagalowsky, A. I.; Cote, R. J.;
543 Lotan, Y., Combination of multiple molecular markers can improve prognostication in patients with
544 locally advanced and lymph node positive bladder cancer. *J Urol* **2010**, *183*, (1), 68-75.
- 545 5. Li, H. X.; Wang, M. R.; Zhao, H.; Cao, J.; Li, C. L.; Pan, Q. J., Comparison of fluorescence in situ
546 hybridization, NMP22 BladderChek, and urinary liquid-based cytology in the detection of bladder
547 urothelial carcinoma. *Diagn Cytopathol* **2013**.
- 548 6. Frantzi, M.; Makridakis, M.; Vlahou, A., Biomarkers for bladder cancer aggressiveness. *Curr*
549 *Opin Urol* **2012**, *22*, (5), 390-6.
- 550 7. Vlahou, A., Back to the future in bladder cancer research. *Expert Rev Proteomics* **2011**, *8*, (3),
551 295-7.
- 552 8. Lotan, Y.; Shariat, S. F.; Schmitz-Drager, B. J.; Sanchez-Carbayo, M.; Jankevicius, F.; Racioppi,
553 M.; Minner, S. J.; Stohr, B.; Bassi, P. F.; Grossman, H. B., Considerations on implementing diagnostic
554 markers into clinical decision making in bladder cancer. *Urol Oncol* **2010**, *28*, (4), 441-8.
- 555 9. Decramer, S.; Gonzalez de Peredo, A.; Breuil, B.; Mischak, H.; Monsarrat, B.; Bascands, J. L.;
556 Schanstra, J. P., Urine in clinical proteomics. *Mol Cell Proteomics* **2008**, *7*, (10), 1850-62.
- 557 10. Zoidakis, J.; Makridakis, M.; Zerefos, P. G.; Bitsika, V.; Esteban, S.; Frantzi, M.; Stravodimos,
558 K.; Anagnou, N. P.; Roubelakis, M. G.; Sanchez-Carbayo, M.; Vlahou, A., Profilin 1 is a potential
559 biomarker for bladder cancer aggressiveness. *Mol Cell Proteomics* **2012**, *11*, (4), M111 009449.
- 560 11. Mischak, H.; Kolch, W.; Aivaliotis, M.; Bouyssie, D.; Court, M.; Dihazi, H.; Dihazi, G. H.;
561 Franke, J.; Garin, J.; Gonzalez de Peredo, A.; Iphofer, A.; Jansch, L.; Lacroix, C.; Makridakis, M.;
562 Masselon, C.; Metzger, J.; Monsarrat, B.; Mrug, M.; Norling, M.; Novak, J.; Pich, A.; Pitt, A.; Bongcam-
563 Rudloff, E.; Siwy, J.; Suzuki, H.; Thongboonkerd, V.; Wang, L. S.; Zoidakis, J.; Zurbig, P.; Schanstra, J.
564 P.; Vlahou, A., Comprehensive human urine standards for comparability and standardization in
565 clinical proteome analysis. *Proteomics Clin Appl* **2010**, *4*, (4), 464-78.
- 566 12. Ruifrok, A. C.; Johnston, D. A., Quantification of histochemical staining by color
567 deconvolution. *Anal Quant Cytol Histol* **2001**, *23*, (4), 291-9.
- 568 13. Siwy, J.; Mullen, W.; Golovko, I.; Franke, J.; Zurbig, P., Human urinary peptide database for
569 multiple disease biomarker discovery. *Proteomics Clin Appl* **2011**, *5*, (5-6), 367-74.
- 570 14. Block, H.; Maertens, B.; Spriestersbach, A.; Brinker, N.; Kubicek, J.; Fabis, R.; Labahn, J.;
571 Schafer, F., Reprint of: Immobilized-Metal Affinity Chromatography (IMAC): A Review. *Protein Expr*
572 *Purif* **2011**.
- 573 15. Beltran, L.; Cutillas, P. R., Advances in phosphopeptide enrichment techniques for
574 phosphoproteomics. *Amino Acids* **2012**, *43*, (3), 1009-24.
- 575 16. Cheung, R. C.; Wong, J. H.; Ng, T. B., Immobilized metal ion affinity chromatography: a
576 review on its applications. *Appl Microbiol Biotechnol* **2012**, *96*, (6), 1411-20.
- 577 17. Reid, C. N.; Stevenson, M.; Abogunrin, F.; Ruddock, M. W.; Emmert-Streib, F.; Lamont, J. V.;
578 Williamson, K. E., Standardization of diagnostic biomarker concentrations in urine: the hematuria
579 caveat. *PLoS One* **2012**, *7*, (12), e53354.

- 1
2
3 580 18. Garapaty, S.; Xu, C. F.; Trojer, P.; Mahajan, M. A.; Neubert, T. A.; Samuels, H. H.,
4 581 Identification and characterization of a novel nuclear protein complex involved in nuclear hormone
5 582 receptor-mediated gene regulation. *J Biol Chem* **2009**, *284*, (12), 7542-52.
- 6 583 19. Roos, P. H.; Jakubowski, N., Methods for the discovery of low-abundance biomarkers for
7 584 urinary bladder cancer in biological fluids. *Bioanalysis* **2010**, *2*, (2), 295-309.
- 8 585 20. Gonzalez-Ortega, O.; Porath, J.; Guzman, R., Adsorption of peptides and small proteins with
9 586 control access polymer permeation to affinity binding sites. Part II: Polymer permeation-ion
10 587 exchange separation adsorbents with polyethylene glycol and strong anion exchange groups. *J*
11 588 *Chromatogr A* **2012**, *1227*, 126-37.
- 12 589 21. Ye, J.; Zhang, X.; Young, C.; Zhao, X.; Hao, Q.; Cheng, L.; Jensen, O. N., Optimized IMAC-IMAC
13 590 protocol for phosphopeptide recovery from complex biological samples. *J Proteome Res* **2010**, *9*, (7),
14 591 3561-73.
- 15 592 22. Feng, S.; Ye, M.; Zhou, H.; Jiang, X.; Zou, H.; Gong, B., Immobilized zirconium ion affinity
16 593 chromatography for specific enrichment of phosphopeptides in phosphoproteome analysis. *Mol Cell*
17 594 *Proteomics* **2007**, *6*, (9), 1656-65.
- 18 595 23. Jeong, S.; Park, Y.; Cho, Y.; Kim, Y. R.; Kim, H. S., Diagnostic values of urine CYFRA21-1,
19 596 NMP22, UBC, and FDP for the detection of bladder cancer. *Clin Chim Acta* **2012**, *414*, 93-100.
- 20 597 24. Memon, A. A.; Chang, J. W.; Oh, B. R.; Yoo, Y. J., Identification of differentially expressed
21 598 proteins during human urinary bladder cancer progression. *Cancer Detect Prev* **2005**, *29*, (3), 249-55.
- 22 599 25. Chen, Y. T.; Chen, C. L.; Chen, H. W.; Chung, T.; Wu, C. C.; Chen, C. D.; Hsu, C. W.; Chen, M.
23 600 C.; Tsui, K. H.; Chang, P. L.; Chang, Y. S.; Yu, J. S., Discovery of novel bladder cancer biomarkers by
24 601 comparative urine proteomics using iTRAQ technology. *J Proteome Res* **2010**, *9*, (11), 5803-15.
- 25 602 26. Gecks, T.; Junker, K.; Franz, M.; Richter, P.; Walther, M.; Voigt, A.; Neri, D.; Kosmehl, H.;
26 603 Wunderlich, H.; Kiehntopf, M.; Berndt, A., B domain containing Tenascin-C: a new urine marker for
27 604 surveillance of patients with urothelial carcinoma of the urinary bladder? *Clin Chim Acta* **2011**, *412*,
28 605 (21-22), 1931-6.
- 29 606 27. Chen, Y. T.; Chen, H. W.; Domanski, D.; Smith, D. S.; Liang, K. H.; Wu, C. C.; Chen, C. L.; Chung,
30 607 T.; Chen, M. C.; Chang, Y. S.; Parker, C. E.; Borchers, C. H.; Yu, J. S., Multiplexed quantification of 63
31 608 proteins in human urine by multiple reaction monitoring-based mass spectrometry for discovery of
32 609 potential bladder cancer biomarkers. *J Proteomics* **2012**, *75*, (12), 3529-45.
- 33 610 28. Eissa, S.; Zohny, S. F.; Shehata, H. H.; Hegazy, M. G.; Salem, A. M.; Esmat, M., Urinary retinoic
34 611 acid receptor-beta2 gene promoter methylation and hyaluronidase activity as noninvasive tests for
35 612 diagnosis of bladder cancer. *Clin Biochem* **2012**, *45*, (6), 402-7.
- 36 613 29. Eissa, S.; Salem, A. M.; Zohny, S. F.; Hegazy, M. G., The diagnostic efficacy of urinary TGF-
37 614 beta1 and VEGF in bladder cancer: comparison with voided urine cytology. *Cancer Biomark* **2007**, *3*,
38 615 (6), 275-85.
- 39 616 30. Oguztuzun, S.; Sezgin, Y.; Yazici, S.; Firat, P.; Ozhavzali, M.; Ozen, H., Expression of
40 617 glutathione-S-transferases isoenzymes and p53 in exfoliated human bladder cancer cells. *Urol Oncol*
41 618 **2011**, *29*, (5), 538-44.
- 42 619 31. Kim, W. J.; Kim, S. K.; Jeong, P.; Yun, S. J.; Cho, I. C.; Kim, I. Y.; Moon, S. K.; Um, H. D.; Choi, Y.
43 620 H., A four-gene signature predicts disease progression in muscle invasive bladder cancer. *Mol Med*
44 621 **2011**, *17*, (5-6), 478-85.
- 45 622 32. Jo, J. O.; Kang, Y. J.; Ock, M. S.; Kleinman, H. K.; Chang, H. K.; Cha, H. J., Thymosin beta4
46 623 expression in human tissues and in tumors using tissue microarrays. *Appl Immunohistochem Mol*
47 624 *Morphol* **2011**, *19*, (2), 160-7.
- 48 625 33. Tran, M. N.; Choi, W.; Wszolek, M. F.; Navai, N.; Lee, I. L.; Nitti, G.; Wen, S.; Flores, E. R.;
49 626 Siefker-Radtke, A.; Czerniak, B.; Dinney, C.; Barton, M.; McConkey, D. J., The p63 Protein Isoform
50 627 DeltaNp63alpha Inhibits Epithelial-Mesenchymal Transition in Human Bladder Cancer Cells: ROLE OF
51 628 MIR-205. *J Biol Chem* **2013**, *288*, (5), 3275-88.

- 1
2
3 629 34. Shiota, M.; Yokomizo, A.; Itsumi, M.; Uchiyumi, T.; Tada, Y.; Song, Y.; Kashiwagi, E.;
4 630 Masubuchi, D.; Naito, S., Twist1 and Y-box-binding protein-1 promote malignant potential in bladder
5 631 cancer cells. *BJU Int* **2011**, 108, (2 Pt 2), E142-9.
- 6 632 35. Higuchi, T.; Shimizu, M.; Owaki, A.; Takahashi, M.; Shinya, E.; Nishimura, T.; Takahashi, H., A
7 633 possible mechanism of intravesical BCG therapy for human bladder carcinoma: involvement of
8 634 innate effector cells for the inhibition of tumor growth. *Cancer Immunol Immunother* **2009**, 58, (8),
9 635 1245-55.
- 10 636 36. Shakoori, A. R.; Hoessli, D. C.; Nasir ud, D., Post-translational modifications in activation and
11 637 inhibition of Oct-1-DNA binding complex in H2B and other diverse gene regulation: prediction of
12 638 interplay sites. *J Cell Biochem* **2013**, 114, (2), 266-74.
- 13 639 37. Lee, H. S.; Park, J. H.; Kim, S. J.; Kwon, S. J.; Kwon, J., A cooperative activation loop among
14 640 SWI/SNF, gamma-H2AX and H3 acetylation for DNA double-strand break repair. *EMBO J* **2010**, 29,
15 641 (8), 1434-45.
- 16 642 38. Mahajan, M. A.; Murray, A.; Samuels, H. H., NRC-interacting factor 1 is a novel cotransducer
17 643 that interacts with and regulates the activity of the nuclear hormone receptor coactivator NRC. *Mol*
18 644 *Cell Biol* **2002**, 22, (19), 6883-94.
- 19 645 39. Garapaty, S.; Mahajan, M. A.; Samuels, H. H., Components of the CCR4-NOT complex
20 646 function as nuclear hormone receptor coactivators via association with the NRC-interacting Factor
21 647 NIF-1. *J Biol Chem* **2008**, 283, (11), 6806-16.
- 22 648 40. Passeron, T.; Valencia, J. C.; Namiki, T.; Vieira, W. D.; Passeron, H.; Miyamura, Y.; Hearing, V.
23 649 J., Upregulation of SOX9 inhibits the growth of human and mouse melanomas and restores their
24 650 sensitivity to retinoic acid. *J Clin Invest* **2009**, 119, (4), 954-63.
- 25 651 41. Protheroe, A. S.; Banks, R. E.; Mzimba, M.; Porter, W. H.; Southgate, J.; Singh, P. N.;
26 652 Bosomworth, M.; Harnden, P.; Smith, P. H.; Whelan, P.; Selby, P. J., Urinary concentrations of the
27 653 soluble adhesion molecule E-cadherin and total protein in patients with bladder cancer. *Br J Cancer*
28 654 **1999**, 80, (1-2), 273-8.
- 29 655 42. Hemmingsen, L.; Rasmussen, F.; Skaarup, P.; Wolf, H., Urinary protein profiles in patients
30 656 with urothelial bladder tumours. *Br J Urol* **1981**, 53, (4), 324-9.
- 31 657 43. Mischak, H.; Allmaier, G.; Apweiler, R.; Attwood, T.; Baumann, M.; Benigni, A.; Bennett, S. E.;
32 658 Bischoff, R.; Bongcam-Rudloff, E.; Capasso, G.; Coon, J. J.; D'Haese, P.; Dominiczak, A. F.; Dakna, M.;
33 659 Dihazi, H.; Ehrich, J. H.; Fernandez-Llama, P.; Fliser, D.; Frokiaer, J.; Garin, J.; Girolami, M.; Hancock,
34 660 W. S.; Haubitz, M.; Hochstrasser, D.; Holman, R. R.; Ioannidis, J. P.; Jankowski, J.; Julian, B. A.; Klein, J.
35 661 B.; Kolch, W.; Luider, T.; Massy, Z.; Mattes, W. B.; Molina, F.; Monsarrat, B.; Novak, J.; Peter, K.;
36 662 Rossing, P.; Sanchez-Carbayo, M.; Schanstra, J. P.; Semmes, O. J.; Spasovski, G.; Theodorescu, D.;
37 663 Thongboonkerd, V.; Vanholder, R.; Veenstra, T. D.; Weissinger, E.; Yamamoto, T.; Vlahou, A.,
38 664 Recommendations for biomarker identification and qualification in clinical proteomics. *Sci Transl*
39 665 *Med* **2010**, 2, (46), 46ps42.
- 40 666 44. Mischak, H.; Ioannidis, J. P.; Argiles, A.; Attwood, T. K.; Bongcam-Rudloff, E.; Broenstrup, M.;
41 667 Charonis, A.; Chrousos, G. P.; Delles, C.; Dominiczak, A.; Dylag, T.; Ehrich, J.; Egido, J.; Findeisen, P.;
42 668 Jankowski, J.; Johnson, R. W.; Julien, B. A.; Lankisch, T.; Leung, H. Y.; Maahs, D.; Magni, F.; Manns, M.
43 669 P.; Manolis, E.; Mayer, G.; Navis, G.; Novak, J.; Ortiz, A.; Persson, F.; Peter, K.; Riese, H. H.; Rossing,
44 670 P.; Sattar, N.; Spasovski, G.; Thongboonkerd, V.; Vanholder, R.; Schanstra, J. P.; Vlahou, A.,
45 671 Implementation of proteomic biomarkers: making it work. *Eur J Clin Invest* **2012**, 42, (9), 1027-36.
- 46 672 45. Vicent, G. P.; Nacht, A. S.; Font-Mateu, J.; Castellano, G.; Gaveglia, L.; Ballare, C.; Beato, M.,
47 673 Four enzymes cooperate to displace histone H1 during the first minute of hormonal gene activation.
48 674 *Genes Dev* **2011**, 25, (8), 845-62.
- 49 675 46. Xiao, A.; Li, H.; Shechter, D.; Ahn, S. H.; Fabrizio, L. A.; Erdjument-Bromage, H.; Ishibe-
50 676 Murakami, S.; Wang, B.; Tempst, P.; Hofmann, K.; Patel, D. J.; Elledge, S. J.; Allis, C. D., WSTF
51 677 regulates the H2A.X DNA damage response via a novel tyrosine kinase activity. *Nature* **2009**, 457,
52 678 (7225), 57-62.
- 53
54
55
56
57
58
59
60

- 1
2
3 679 47. Ogiwara, H.; Ui, A.; Otsuka, A.; Satoh, H.; Yokomi, I.; Nakajima, S.; Yasui, A.; Yokota, J.;
4 680 Kohno, T., Histone acetylation by CBP and p300 at double-strand break sites facilitates SWI/SNF
5 681 chromatin remodeling and the recruitment of non-homologous end joining factors. *Oncogene* **2011**,
6 682 30, (18), 2135-46.
7 683 48. Holland, D. G.; Burleigh, A.; Git, A.; Goldgraben, M. A.; Perez-Mancera, P. A.; Chin, S. F.;
8 684 Hurtado, A.; Bruna, A.; Ali, H. R.; Greenwood, W.; Dunning, M. J.; Samarajiwa, S.; Menon, S.; Rueda,
9 685 O. M.; Lynch, A. G.; McKinney, S.; Ellis, I. O.; Eaves, C. J.; Carroll, J. S.; Curtis, C.; Aparicio, S.; Caldas,
10 686 C., ZNF703 is a common Luminal B breast cancer oncogene that differentially regulates luminal and
11 687 basal progenitors in human mammary epithelium. *EMBO Mol Med* **2011**, 3, (3), 167-80.
12 688 49. Kim, T. H.; Chiera, S. L.; Linder, K. E.; Trempus, C. S.; Smart, R. C.; Horowitz, J. M.,
13 689 Overexpression of transcription factor sp2 inhibits epidermal differentiation and increases
14 690 susceptibility to wound- and carcinogen-induced tumorigenesis. *Cancer Res* **2010**, 70, (21), 8507-16.
15 691 50. Segil, N.; Roberts, S. B.; Heintz, N., Mitotic phosphorylation of the Oct-1 homeodomain and
16 692 regulation of Oct-1 DNA binding activity. *Science* **1991**, 254, (5039), 1814-6.
17 693 51. Maddox, J.; Shakya, A.; South, S.; Shelton, D.; Andersen, J. N.; Chidester, S.; Kang, J.;
18 694 Gligorich, K. M.; Jones, D. A.; Spangrude, G. J.; Welm, B. E.; Tantin, D., Transcription factor Oct1 is a
19 695 somatic and cancer stem cell determinant. *PLoS Genet* **2012**, 8, (11), e1003048.
20 696 52. Yoshikawa, M.; Mukai, Y.; Okada, Y.; Tsumori, Y.; Tsunoda, S. I.; Tsutsumi, Y.; Aird, W. C.;
21 697 Yoshioka, Y.; Okada, N.; Doi, T.; Nakagawa, S., Robo4 is an effective tumor endothelial marker for
22 698 antibody-drug conjugates based on the rapid isolation of the anti-Robo4 cell-internalizing antibody.
23 699 *Blood* **2013**.
24 700 53. Chen, W. F.; Gao, W. D.; Li, Q. L.; Zhou, P. H.; Xu, M. D.; Yao, L. Q., SLIT2 inhibits cell
25 701 migration in colorectal cancer through the AKT-GSK3beta signaling pathway. *Int J Colorectal Dis*
26 702 **2013**.
27 703 54. El Hour, M.; Moncada-Pazos, A.; Blacher, S.; Masset, A.; Cal, S.; Berndt, S.; Detilleux, J.; Host,
28 704 L.; Obaya, A. J.; Maillard, C.; Foidart, J. M.; Ectors, F.; Noel, A.; Lopez-Otin, C., Higher sensitivity of
29 705 Adamts12-deficient mice to tumor growth and angiogenesis. *Oncogene* **2010**, 29, (20), 3025-32.
30 706 55. Minder, P.; Bayha, E.; Becker-Pauly, C.; Sterchi, E. E., Meprinalpha transactivates the
31 707 epidermal growth factor receptor (EGFR) via ligand shedding, thereby enhancing colorectal cancer
32 708 cell proliferation and migration. *J Biol Chem* **2012**, 287, (42), 35201-11.

709

710

711

712

713

714

715

716

717

718

Table 1. Pearson Correlation analysis for H2B and Zn finger protein 335/NIF-1 based on the respective OD values from the same tissue specimens. An inverse correlation of the tissue levels of the two proteins is predicted.

Correlation : NIF-1 & H2B mean optical density

		H2B Optical Density	NIF-1 Optical Density
H2B Optical Density	Pearson Correlation	1	-,391*
	Sig. (2-tailed)		,036
	N	29	29
NIF-1 Optical Density	Pearson Correlation	-,391*	1
	Sig. (2-tailed)	,036	
	N	29	29

*. Correlation is significant at the 0.05 level (2-tailed).

719

Table 2. Short-list of promising candidates among the peptidomics findings meriting further investigation. Selection was based on strength of evidence for differential expression in the discovery phase (e.g. selective presence in specific stages, number of samples expressing the peptide etc.) but also presumed functional relevance to BC in combination to lack of existing association with BC, based on existing knowledge.

	Protein	Stage Identified	Reported Function
1	Bromodomain adjacent to zinc finger domain protein 2B	T2+	Transcription regulation, DNA damage response, Regulation of H2A.X ⁴⁶
2	Histone acetyltransferase p300	B	Chromatin remodeling –Removal of H2A-H2B dimers DNA damage response ⁴⁷
3	Zinc finger protein 703	T2+	Transcription regulation, Breast cancer oncogene ⁴⁸
4	Transcription factor Sp2	T1	Zinc associated transcription factor, Oncogene ⁴⁹
5	POU domain, class 2, transcription factor 1	T1	H2B regulation, Somatic and cancer stem cell identity ^{50, 51}
6	Roundabout homolog 4	T1,T2+	Slit protein Receptor – Angiogenesis, Tumour vascular targeting ⁵²
7	Slit homolog 2	T1	Inhibition of cell migration ⁵³
8	A disintegrin and metalloproteinase with thrombospondin motifs 12	T1	Zinc Metalloprotease, Tissue remodelling & Angiogenesis ⁵⁴
9	Meprin A subunit alpha	T1	Zinc Metalloprotease. Pro-angiogenic & Pro-migratory activity ⁵⁵

1
2
3 720
4
5

6 721 **Figure legends**

7
8
9 722 **Figure 1.** Schematic representation of the study design.
10
11

12 723
13
14

15 724 **Figure 2.** (Precursor))Protein classification of the received identifications based on protein
16
17 725 biological function. Classification in 13 categories was conducted (based on GO and Medline
18
19 726 search) that include: immune response, cytoskeleton arrangement, ECM and cell adhesion
20
21 727 associated proteins, metabolic processes, transport, stress response, proliferation and/or
22
23 728 apoptosis, differentiation, transcription regulation, chromatin remodelling, proteolysis and
24
25 729 signal transduction.
26
27

28 730
29

30 731 **Figure 3.** (A) Zn finger protein 335/ NIF-1 and (B) H2B ELISA data, following analysis of a
31
32 732 total number of 158 (NIF-1) and 147 (H2B) urine samples. Mean values, standard deviation
33
34 733 and number of positive samples for the different categories and respective box plots are
35
36 734 shown (raw data per sample are provided in **Supplementary Table 3**).
37
38

39 735
40
41

42
43 736 **Figure 4.** Representative images from immunohistochemical analysis of BC tissue sections
44
45 737 and respective quantification of (A) Zn finger protein 335/NIF-1 and (B) H2B expression. A
46
47 738 colour deconvolution plugin from Image J software enabled the quantitation of signal
48
49 739 intensity between the different BC stages .
50

51
52 740 * : statistical significant difference
53
54

55 741
56
57

58 742
59
60

743

744 **Supplementary Table 1.** Clinical information for urine and tissue samples used in the study.

745 Three xls sheets are included, one for each of the different studies: “Urine samples employed
746 in LCMS” (discovery set); “Urine samples employed in Elisa” (verification set) ; “BC Tissue
747 specimens” (IHC set)

748 **Supplementary Table 2.** List of urinary peptides and precursor proteins identified following
749 IMAC fractionation and LC-MS/MS. Two xls sheets are included: “Peptides” showing the
750 MS identifiers for each peptide and “Proteins” summarizing list if precursor proteins and
751 respective functional annotation analysis.

752 **Supplementary Table 3.** Urinary ELISA data and immunohistochemical measurements for
753 NIF-1 and H2B per sample. Three xls sheets are included: “Elisa data” showing values per
754 sample and graphs following different normalization means ; “IHC values and graphs”
755 showing mean measurements in reference to different grading systems; and “IHC-Image J
756 calculations” showing intensity measurements per image and section.

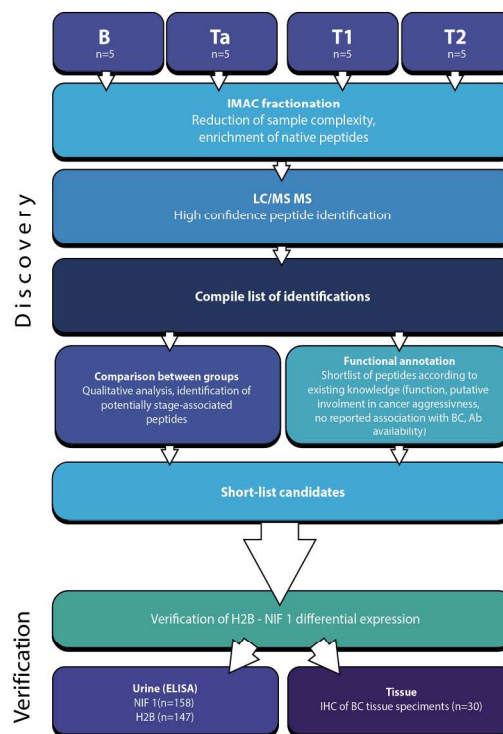
757

758 **Supplementary Figure legend**

759 **Supplementary Figure 1.** Images acquired following staining of bladder cancer tissue
760 specimens for H2B and NIF-1, and representing cases of intensity deviations (from the mean
761 throughout the section). Variations in intensity measurements are usually associated with
762 biological variability within the same section, (e.g. different nuclei morphology, staining
763 intensity per cell) reflecting more likely differences in the degree of aggressiveness of the
764 cancer cells.

765

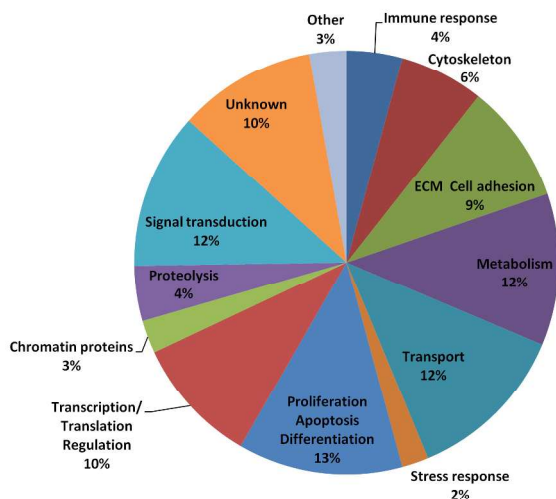
Figure 1



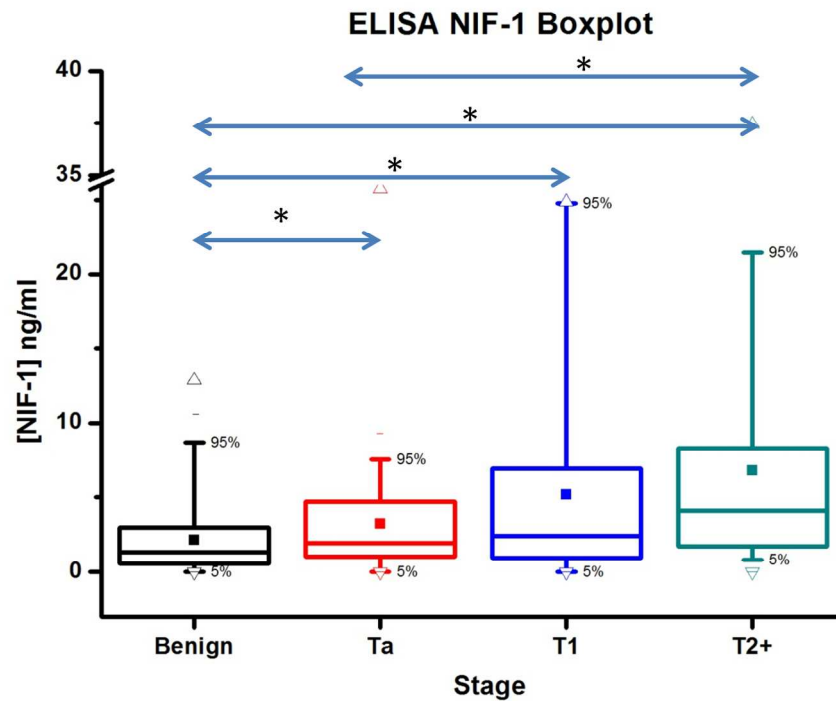
254x190mm (300 x 300 DPI)

1
2
3
4
5
6
7
8
9
10
11
12
13
14
15
16
17
18
19
20
21
22
23
24
25
26
27
28
29
30
31
32
33
34
35
36
37
38
39
40
41
42
43
44
45
46
47
48
49
50
51
52
53
54
55
56
57
58
59
60

Figure 2

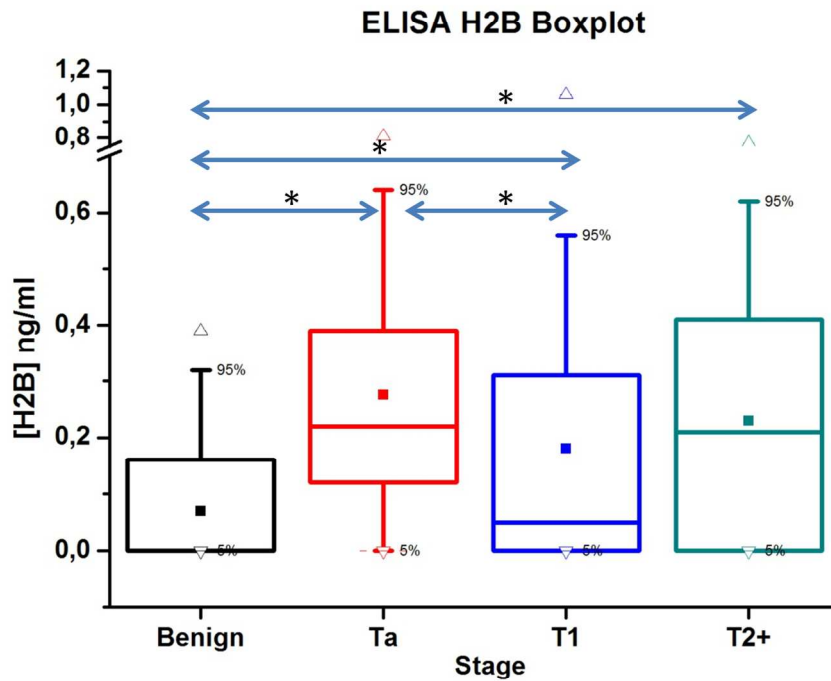


254x190mm (300 x 300 DPI)



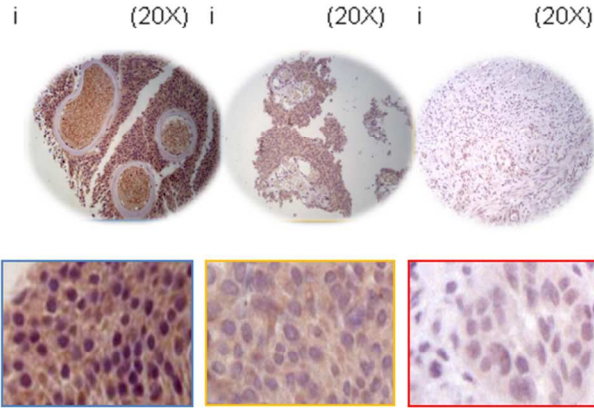
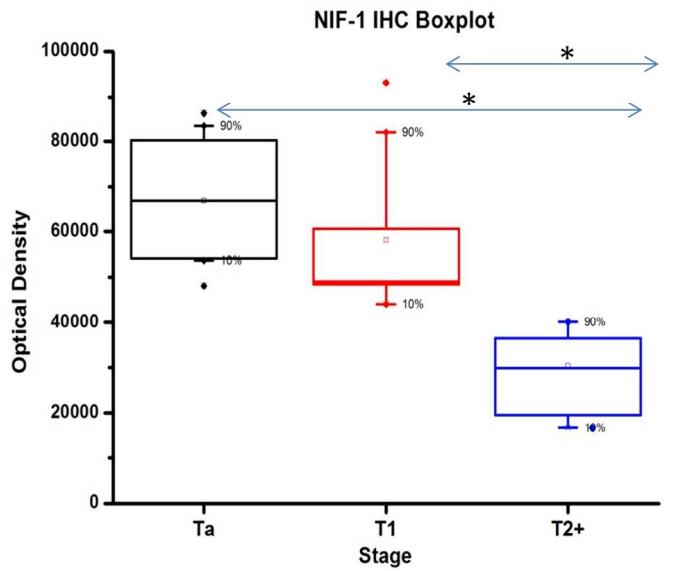
	n	[NIF-1] ng/ml	st.dev	Positive
Benign	47	2,19	2,73	38/47
Ta	44	3,26	4,11	42/44
T1	36	5,19	6,48	34/36
T2+	31	6,80	7,97	30/31

154x190mm (300 x 300 DPI)



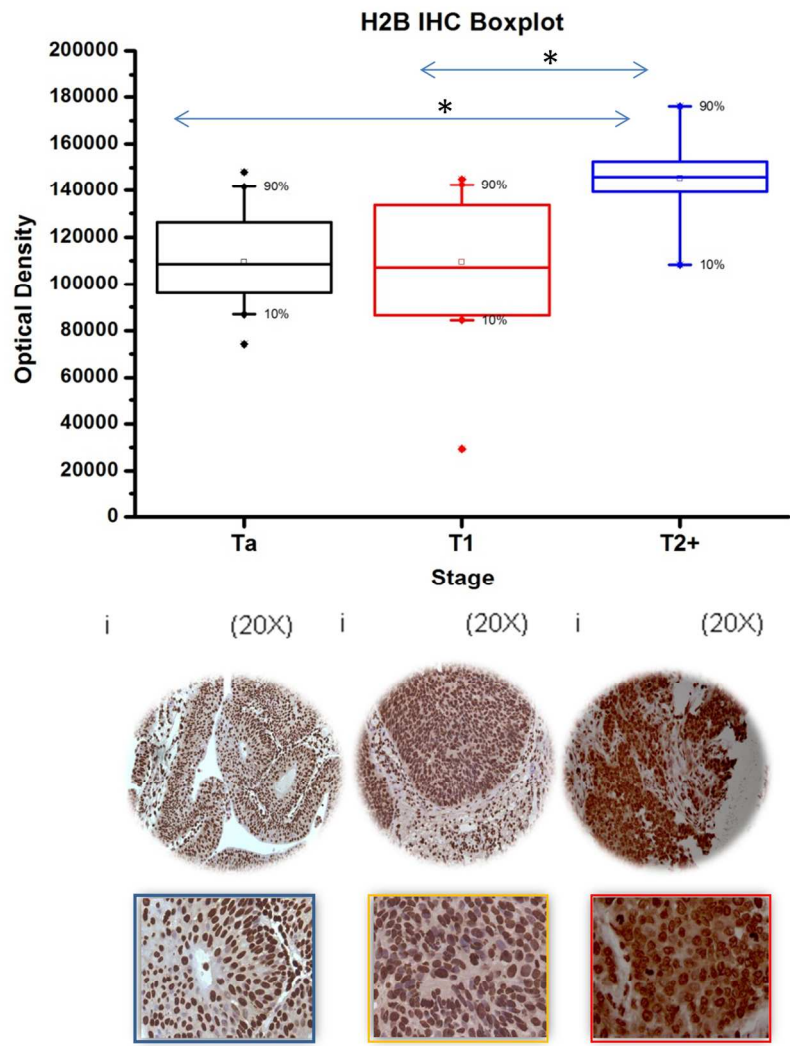
	n	[H2B] ng/ml	st.dev	Positive
Benign	39	0,069	0,111	15/39
Ta	40	0,262	0,212	35/40
T1	36	0,181	0,235	19/36
T2+	32	0,230	0,223	23/32

149x190mm (300 x 300 DPI)

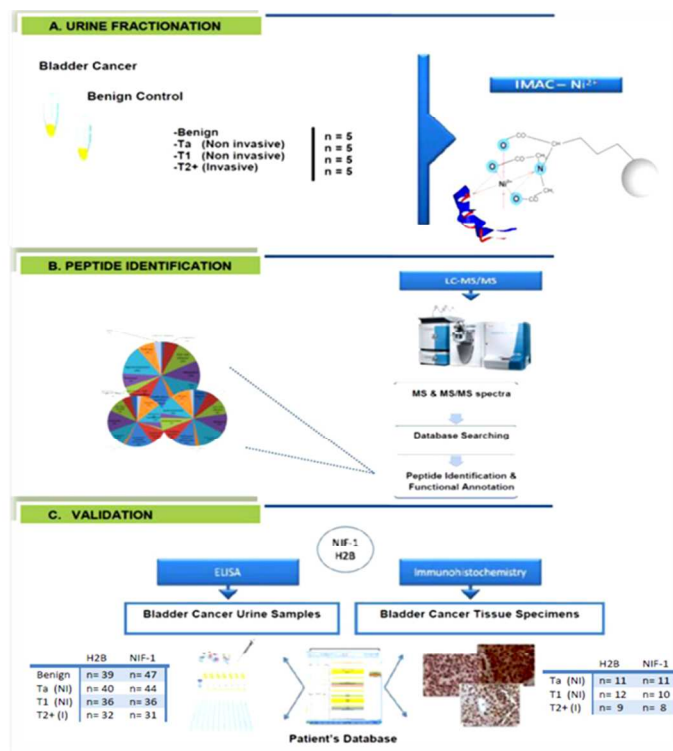


173x186mm (300 x 300 DPI)

1
2
3
4
5
6
7
8
9
10
11
12
13
14
15
16
17
18
19
20
21
22
23
24
25
26
27
28
29
30
31
32
33
34
35
36
37
38
39
40
41
42
43
44
45
46
47
48
49
50
51
52
53
54
55
56
57
58
59
60



161x176mm (300 x 300 DPI)



81x60mm (300 x 300 DPI)